Elżbieta PIECZYSKA*, Hisaaki TOBUSHI**

TiNi SHAPE MEMORY ALLOY TENSION AT VARIOUS TEMPERATURES – INFRARED IMAGING OF SHAPE MEMORY EFFECT AND PSEUDOELASTICITY

SUMMARY

The mechanical characteristics and the infrared imaging of stress-induced martensite transformation developing in TiNi shape memory alloy (SMA) subjected to tension in various conditions with respect to the SMA austenite finish parameter have been presented. Based on the mechanical curves and their related temperature changes it was found that onset of the martensitic transformation appears at the end of the elastic part of the stress-strain curve, since the temperature starts to increase before the knee in the curve. The uniform temperature distribution observed on the specimen surface at this stage confirms that the initial martensite transformation is macroscopically homogeneous. For the shape memory effect behavior the uniform temperature distribution on the specimen surface was observed during the complete process of the SMA loading which means that the transformation process is macroscopically homogeneous. For the shape memory alloy pseudoelasticity behavior bands of higher temperature have been recorded during the specimen loading and bands of lower temperature during its unloading, manifesting localized Lüders-like deformation, caused by the transformation process. As the transformation advances, the higher temperature changes have been recorded. Taking advantages from the infrared technique a new results concerning nucleation and development of the martensite forward and reverse transformation have been obtained. Finally, some examples of the SMA new applications due to the SMA shape memory effect have been presented and discussed.

Keywords*: shape memory alloy, TiNi, martensite transformation, shape memory effect, pseudoelasticity*

BADANIE STOPU TiNi Z PAMIĘCIĄ KSZTAŁTU W PROCESIE ROZCIĄGANIA W RÓŻNYCH TEMPERATURACH – EFEKT PAMIĘCI KSZTAŁTU I PSEUDOSPRĘŻYSTOŚĆ W TECHNICE BADAŃ W PODCZERWIENI

W pracy omówiono właściwości stopów z pamięcią kształtu, przedstawiono wyniki własnych badań parametrów mechanicznych w procesie jednoosiowego rozciągania oraz zmian temperatury próbek, otrzymane w sposób bezstykowy za pomocą kamery termowizyjnej o wysokiej czułości. Na podstawie charakterystyk mechanicznych oraz zmian temperatury próbek tego stopu stwierdzono, że indukowana naprężeniem przemiana fazowa inicjuje się pod koniec zakresu sprężystego, zdecydowanie przed plateau, charakterystycznym dla przebiegu przemiany. Zarejestrowane rozkłady zmian temperatury na powierzchni obciążanych próbek pozwoliły wykazać, że przemiana martenzytyczna wprost i odwrotna, odpowiedzialna za pseudosprężystość SMA, zachodzi w sposób niejednorodny. Inicjuje się w postaci cienkich pasm, podobnych do pasm Lüdersa, które następnie rozwijają się w dwóch prawie prostopadłych kierunkach. Niejednorodność przebiegu przemiany martenzytycznej udokumentowano w technice badań w podczerwieni oraz fotografując relief na powierzchni próbki. Omówiono przykłady nowych zastosowań stopu z pamięcią kształtu.

Słowa kluczowe*: stop z pamięcią kształtu, TiNi, przemiana martenzytyczna, efekt pamięci kształtu, pseudosprężystość*

1. INTRODUCTION TO SHAPE MEMORY ALLOYS

The development of intelligent or smart materials and their systems is highly anticipated since they have various functions, such as sensing, working and crack-healing by themselves, etc. In the field of intelligent materials, the development of shape memory alloy has attracted high attention since the unique properties of the shape memory effect (SME) and superelasticity (SE) appears (Tobushi, 2009). If we use the SME and SE in practical applications, not only large recovery strain but also high recovery stress, energy storage and energy dissipation can be obtained. Successful applications of shape memory effect are couplings, actuators in electric appliances, automobile devices, robots and smart materials, e.g. composites with polymer or metal matrix. Pseudoelasticity and high elasticity are applied to orthodontic arch wire, antennas for cellular phones, guide wires for catheters, medical instruments, orthopedic devices, etc. (Shaw 1997, Dutkiewicz 2008, Tobushi 2009).

The shape memory alloy deformation behavior under various conditions is related to many practical applications, and is summarized graphically by the three-dimensional stress-strain-temperature diagram in Figure 1.

* Institute of Fundamental Technological Research, Pawinskiego 5B, 02-106 Warsaw, Poland
** Aichi Institute of Technology, 1247 Yachigusa, Yakusa-cho, Toyota, 470-0392, Japan

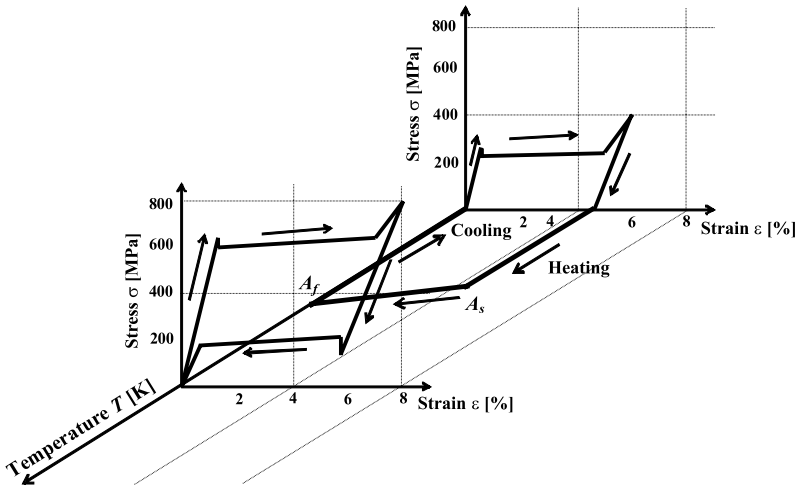

Fig. 1. Three-dimensional stress-strain-temperature diagram showing the deformation and shape memory and superelastic behaviors of a TiNi alloy deformed below A_s and above A_f

In the Figure 1, A_s and A_f denote the austenite start and finish temperatures, respectively. In the yield stage of the stress-strain diagram shown in the σ–ε plane, the deformation accompanied by the stress plateau appears due to the martensitic transformation. This phenomenon is called the stress-induced martensitic transformation. The strain induced at a temperature below A_s, 6%, recovers between A_s and A_f after the applied stress has been removed and the specimen heated, as seen in the ε–T plane, showing the shape memory effect (Figs 3, 4). At a temperature above A_f the martensite transformation is developing, leading to the usual superelastic loop with upper and lower plateaus (Figs 5, 7, 8).

The main features of the SME and SE are induced due to the twinning, martensitic transformation and the martensite variants reorientation. Since the shape memory alloys are very sensitive to the temperature change, effects of thermomechanical couplings related to the stress-induced martensite transformation responsible for their behavior and related to many effective applications can be studied on the basis of the obtained mechanical and temperature characteristics.

2. MATERIAL AND EXPERIMENTAL PROCEDURE

The experiments have been carried out on two kinds of TiNi shape memory alloy belt specimens of 160 × 10 × 0.4 mm, cut from strips; characterized by the A_f temperature equal to 333 K and 283 K, respectively. The specimens have been subjected to the strain-controlled tension test on the Instron testing machine in quasi-static range of strain rates. In the course of the investigation both the mechanical characteristics and the distribution of the infrared radiation emitted by the specimen surface were registered continuously. The diagram of the experimental equipment is presented in Figure 2. The infrared camera used is a long wave type, working in the wave range of 7.5–13 μm. The matrix size is 320 × 240 pixels. The spatial and the temperature resolutions depend on the camera-specimen distance. In the case of the results presented here, the distance was 10 cm and the spatial resolution was 0.3 mm. Before the testing, the specimen surface was covered with a very thin layer of a carbon powder in order to make its emissivity higher and more homogeneous. The specimen mean temperature was calculated over an area of 8 mm × 60 mm, located in the central part of the specimen. The obtained stress-strain characteristics, the specimen temperature distribution and the mean temperature changes enable the study of the process of nucleation and the further development of the martensitic forward and reverse transformation, which are responsible for the shape memory alloy thermomechanical behavior. The latter is important in the SMA number of emerging practical applications.

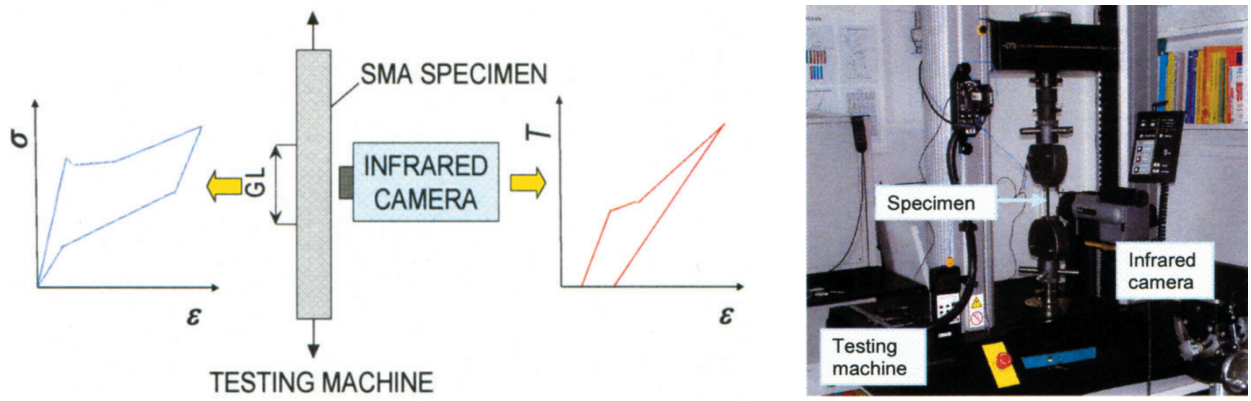

Fig. 2. Diagram and photograph of experimental equipment for mechanical and temperature investigation

The mean temperature, calculated from the specimen surface, is usually used in the presented curves and thermo-mechanical coupling analysis (Fig. 7). The measurement temperature accuracy obtained for the used infrared camera was approximately 0.2 K.

3. INFRARED IMAGING OF STRESS-INDUCED TRANSFORMATION

Investigations of the temperature variations accompanying the martensite transformation processes in shape memory alloys by infrared camera have been launched quite recently (Shaw 1997). At first, the temperature was estimated using a thermocouple, which, however, was limited to the measurement at a single chosen point. A modern infrared camera is very useful in the investigations, since it allows for monitoring of the temperature distribution on the examined specimen surface and the calculation of the mean temperature in a contact-less way over arbitrarily chosen area, segment or a number of points The stress-induced martensitic transformation manifests an exothermic character, while the reverse shows endothermic transformation, so during loading the SMA temperature increases and during unloading the temperature decreases (Show 1997, Gadaj 2002, Pieczyska 2004, 2006).

The measured temperature changes depend on the strain rate; the higher the strain rate, the higher the temperature change. The recorded maximal temperature increments were of about 4K for the strain rate 10^{-4} s^{-1} to about 40 K for 10^{-1}s^{-1} (Pieczyska 2008). During the SMA loading process, the recorded temperature distribution was more or less uniform. It means that the process of the phase transformation, analyzed in macro-scale, was more or less homogeneous (Brinson 2004, Favier 2007, Pieczyska 2004, 2008, 2010, He 2010).

Depending on the test temperature in reference to the SMA austenite finish (A_f) and austenite start (A_s) temperature parameters, the recorded temperature distribution is more or less uniform. The stress-strain curves and the specimen temperature distributions obtained during tension of the TiNi SMA at the temperature below, at and above A_f are shown in Figures 3–5, 7 and 8.

3.1. Infrared imaging of the shape memory effect

Figure 3 presents the stress-strain curve and the specimen temperature distributions obtained during tension of the TiNi SMA (A_s=320 K, A_f=333 K) performed at 295 K (below the SMA austenite start temperature, i.e. registering shape memory effect. The images presented on the right show the specimen temperature distribution recorded at the strains equal to 0,1%, 2%, 3% during loading; and 2.9% during unloading, respectively.

From the Figure 3 one can observe that the specimen temperature increases during the SMA loading and decreases

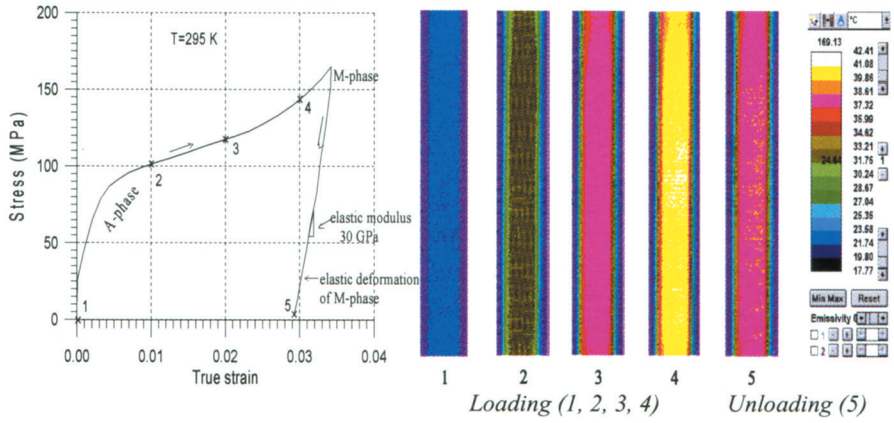

Fig. 3. Stress-strain curve and temperature distribution on the surface of TiNi SMA tape obtained at various strains under strain rate of 1.87×10^{-3}s^{-1} during loading and unloading at T < A_s studied by infrared thermography

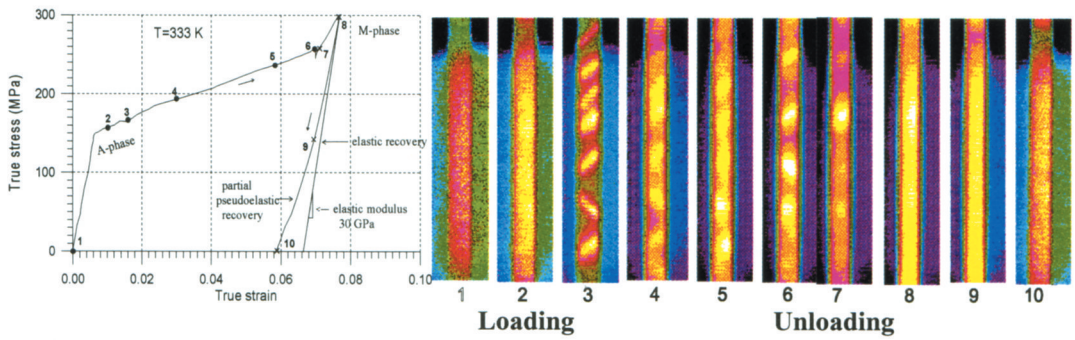

Fig. 4. Stress-strain curve and temperature distribution on the surface of TiNi SMA tape at various strains under strain rate of 1.87×10^{-3}s^{-1} during loading and unloading at $T = A_f$ studied by infrared thermography

during the unloading but that the recorded temperature distribution is uniform, i.e. the transformation process observed in macro-scale by the applied infrared equipment is homogeneous. After unloading, a great residual strain ≈3% called also the shape memory effect was recorded. The specimen recovers its former size and shape during its subsequent heating at the temperature between 320 K and 333 K.

The stress-strain curve and the temperature distribution accompanying the SMA tension performed at $T = A_f$ (333 K) with the strain rate equal to 1.87×10^{-3} s^{-1} is presented in Figure 4.

Looking at the Figure one can notice that the temperature distribution of the SMA loading by tension at $T = A_f$ is not uniform, especially during the loading, manifesting that the martensite transformation process is not homogeneous. Namely, bands of the new phase, related to the higher temperatures, nucleate at various positions and grow wider thereafter on the whole specimen surface.

Moreover, one should also take into account that the results presented in Figures 3 and 4 were obtained for the similar specimen of the shape memory alloy during tension carried out with the same strain rate 1.87×10^{-3} s^{-1}, however in Figure 3 the specimen was subjected to tension in the strain range of about 4%, while in Figure 4 twice higher strain range, approximately 8%, was applied.

3.2. Infrared imaging of the shape memory alloy pseudoelastic behavior

For the TiNi SMA characterized by A_f = 283 K and loading by tension in room conditions (295 K) the temperature imaging is much more complex (Figs 5, 8), reflecting the much more complex transformation process. The results, presented in Figure 5, were obtained for the tension carried out with higher strain rate equal to 1.6×10^{-2} s^{-1} and within the strain range approximately 6%. For the test, a superelastic (pseudoelastic) behavior was recorded and much higher stresses over 500 MPa have been achieved in the range of the martensite forward transformation in comparison to the formerly obtained results: 150–260 MPa (Figs 3 and 4). After the unloading, only a small residual strain has been recorded (Fig. 5, left). Moreover, one can observe a localized *Lüders*-like deformation developing in the SMA specimen. The temperature distribution recorded on the specimen surface reflects immediately a nucleation and development of the new phases, both martensite and reverse, due to the temperature changes and significant temperature variations between the parent and the new phase. Namely, bands of significantly higher temperature, corresponding to the exothermic inhomogeneous martensite forward transformation, started from the grip area were recorded during the SMA loading, whereas bands of significantly lower temperature, corresponding to the endothermic reverse transformation, were recorded during the unloading process. It was observed that in the case of high strain rate, the transformation bands nucleate not only at the ends or center, but also at various positions and develop thereafter on the whole surface of the specimen (Pieczyska 2008, 2010, He 2010).

Sometimes the nucleation and growth of the transformation bands are so clear and significant that they can be observed directly on the surface of the specimen with the naked eye (Fig. 6). Such effects were obtained with the test for which stress-strain curve and infrared imaging are presented in Figure 5.

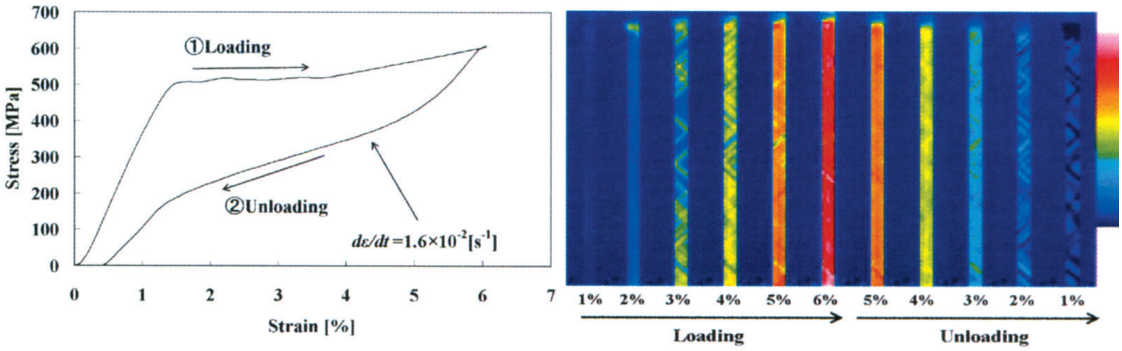

Fig. 5. Stress-strain curve and temperature distribution on surface of TiNi SMA specimen at various strains under a strain rate of 1.6×10^{-2}s^{-1} during loading and unloading at $T > A_f$ studied by infrared thermography

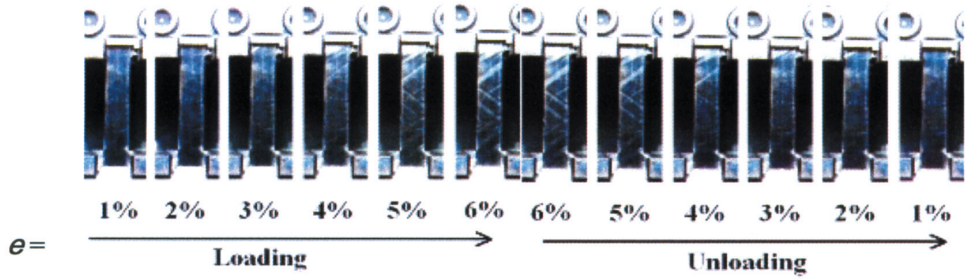

Fig. 6. Deformation patterns on TiNi SMA specimen surface due to phase transformations in tension test under strain rate = 1.6×10^{-2} s^{-1}

Stress-strain and temperature-strain curves obtained during TiNi SMA pseudoelastic behavior with strain rate 10^{-2} s^{-1} is shown in Figure 7.

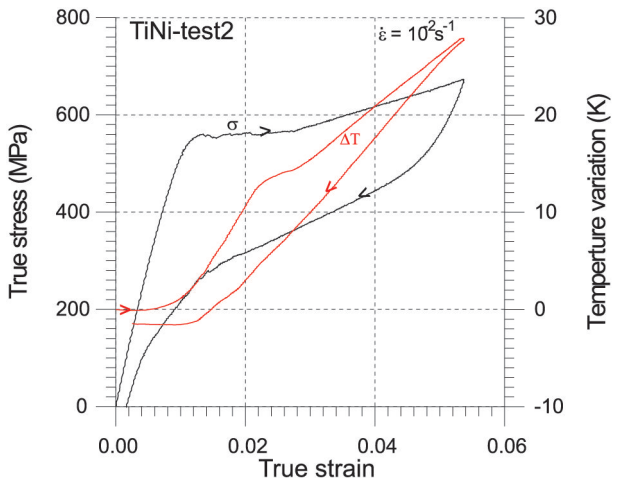

Fig. 7. Stress- and temperature-strain curves obtained for TiNi tension test performed with strain rate 10^{-2} s^{-1}

Looking at the mechanical and the temperature graphs obtained for the strain rate 10^{-2} s^{-1} and for the strain range 8% presented in Figure 7 one can conclude that the martensite transformation during the loading processes is almost completed. Moreover, one can find from the presented data that the martensite transformation starts when the onset in temperature is recorded and the transformation is developed until the temperature does not increase (during the latest loading stage).

The temperature distributions on the specimen surface (thermograms) obtained during the test were overlapped on the stress- and the temperature-strain diagram and presented in Figure 8, (Pieczyska, 2008).

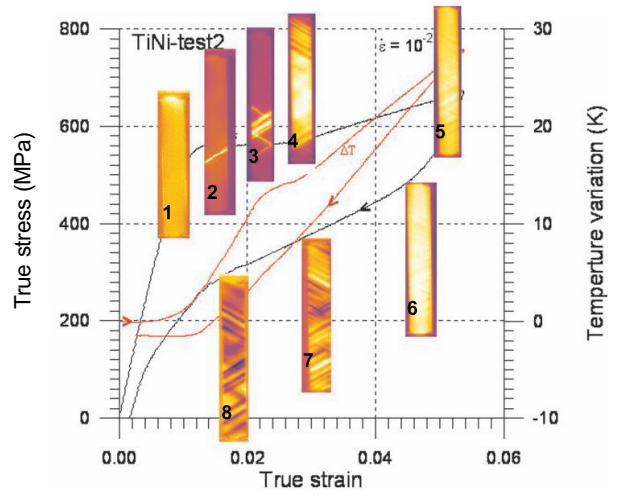

Fig. 8. Stress- and temperature-strain curves supplemented by the infrared temperature distributions obtained for TiNi SMA tension test performed with strain rate 10^{-2} s^{-1}: thermograms 1–5 loading; 6–8 unloading

One can notice that transformation bands of significantly higher temperature are corresponding to the exothermic inhomogeneous martensitic forward transformation recorded during the SMA loading (thermograms 1–5), whereas bands of significantly lower temperature, corresponding to the endothermic reverse transformation, were recorded during the specimen unloading (thermograms 6–8). As the tension proceeds the band widens significantly and other bands appear, at first parallel and then inclined at the same angle but developing in the opposite direction (Pieczyska 2006). As the strain increases, more and more transformation bands appear and move towards the specimen grip. When the bands reach the grips area (Fig. 8, thermogram 4), the upswing region on both the stress- and the temperature-strain curves are observed, reflecting the more advanced stage of the transformation process. The stress and the temperature increase fast, however the temperature distribution becomes more uniform at more advanced transformation stage (5), so the transformation process seems to be more homogeneous, probably due to the transferring heat overlapping effects.

During the unloading, after passing the elastic stage (Fig. 8, thermogram 6), the reverse transition takes place. After the unloading is completed, the material almost returns to its parent austenite phase. However, the temperature drops below its initial value and the residual strains, related to a small amount of the martensitic and irreversible macro-structural changes appear, depending on the specimen history (Brinson 2004, Pieczyska 2006, Favier 2007).

The phenomena of localized Lüders-like transformations accompanying the complete loop of the TiNi SMA pseudoelasticity behavior analyzed in infrared technique have been confirmed by (Murusawa 2004, Daly 2007) by using a Digital Image Correlation (DIC) Strain Map technique.

4. NEW APPLICATIONS OF SMA SHAPE MEMORY EFFECT AND SUPERELASTICITY

Due to unique properties of shape memory alloys manifested in various conditions many projects are still developing for daily life, medicine and technology practical applications.

4.1. Solar vehicle and engine based on SMA shape memory effect

A photograph of a solar-powered car driven by a simple-pulley TiNi SMA heat engine is shown in Figure 9.

The SMA heat engine is driven by the sun light using a Fresnel lens. In the SMA heat engine, two pulleys are connected by the SMA belt which is shape-memorized into the flat plane by the heat treatment before making into a loop by welding. The car moves based on the recovery force in the SMA belt which appears by heating from the sun light focused by the Fresnel lens. From a view-point of global warming prevention, being able to use the low-temperature thermal energy around 373 K, the development of the compact and harmless clean SMA heat engine is greatly anticipated.

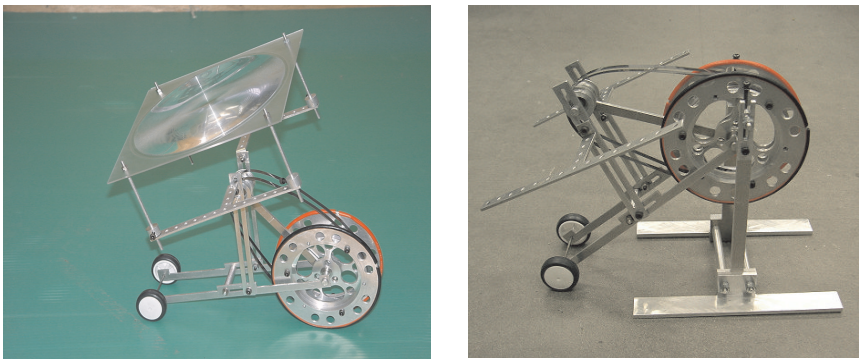

Fig. 9. Project of SMA new solar vehicle and engine using a shape memory effect (SME); AIT

4.2. Shape memory alloy new engine

A design of a new shape memory alloy engine proposed by the Aichi Institite of Technology students is shown in Figure 10.

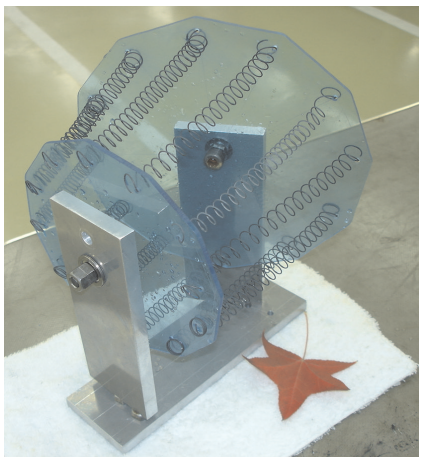

Fig. 10. Photograph of design of SMA engine using a SME and driven by a hot water; AIT

The springs made from TiNi SMA are in martensite state in room conditions. When the engine is partly put into a hot water, above the SMA A_F temperature, those SMA springs which are immersed in the hot water are suddenly shrinking, and the device starts to rotate.

5. CONCLUSIONS

The mechanical characteristics, the temperature changes and the infrared imaging of stress-induced martensite transformation occurring in TiNi SMA subjected to tension in various conditions with respect to the alloy austenite finish temperature have been presented. Based on the mechanical curves and their related temperature changes it was found that an onset of the martensitic transformation appears at the end of the elastic part of the stress-strain curve, since the temperature starts increase before the knee in the curve. The uniform temperature distribution observed on the specimen surface at this stage confirms that the initial martensite transformation is macroscopically homogeneous. At higher strains, for the shape memory alloy pseudoelastic behavior, bands of higher temperature are observed during the specimen loading and bands of lower temperature during its unloading, manifesting localized Lüders-like transformation. When the transformation bands reach the grips area during the loading, an upswing effects on both the stress-strain and the temperature-strain curves are observed, reflecting the intense process of the advanced martensite transformation. For the shape memory effect behavior the uniform temperature distribution on the specimen surface is observed till the end of the loading which means that the transformation process is macroscopily homogeneous. Using a modern, sensitive and fast infrared camera enables to obtain new results of the nucleation and development of the martensite forward and reverse transformations. Due to unique properties of shape memory alloys manifested in various conditions, many practical applications are still developing, for daily life, medicine and technology.

Acknowledgments

The research has been carried out with support of the Polish Ministry of Science and Higher Education under Grant No 501220837, the Japan Society for the Promotion of Science (JSPS); Post-doc ID P04774 and Scientific Research (C) No 18560090 and The Naito Research Grant.

References

Tobushi H., Pieczyska E.A., Ejiri Y. and Sakuragi T. 2009, *Thermomechanical Properties of Shape-Memory Alloy and Polymer and their Composite*. Mechanics of Advanced Materials and Structures, vol. 16, pp. 236–247.

Pieczyska E. 2008, *Analiza doświadczalna właściwości termomechanicznych stopów TiNi oraz poliuretanu z pamięcią kształtu*. Prace IPPT/IFTR Reports, ISBN 978-83-89687-37-1, 3, (in Polish, graphs in English).

Shaw J.A., Kyriakides S. 1997, *On the nucleation and propagation of phase transformation fronts in a TiNi Alloy*. Acta Materiala, 45, 2, pp. 683–700.

Gadaj S.P., Nowacki W.K., Pieczyska E.A. 2002, *Temperature evolution in deformed shape memory alloy*. Infrared Physics & Tech., 43, pp. 151–155.

Pieczyska E.A., Gadaj S.P., Nowacki W.K., Tobushi H. 2004, *Thermomechanical Investigations of Martensite and Reverse Transformations in TiNi Shape Memory Alloy*. Bull. Pol. A . Sci Tech Sci 52 (3), pp. 165–171.

Pieczyska E.A., Gadaj S.P., Nowacki W.K., Tobushi H. 2006, *Phase transformation front evolution for stress- and strain-controlled test in TiNi SMA*. Experimental Mechanics, vol. 46, No 4, pp. 531–542.

Dutkiewicz J.M., Maziarz W., Czeppe T., Lityńska L., Nowacki W.K., Gadaj S.P., Luckner J., Pieczyska E.A. 2008, *Powder metallurgy technology of NiTi shape memory alloy*. Eur. Phys. J., 158, pp. 59–65.

Murasawa G., Koushinbou M., Yoneyama S., Sakuma T., Takashi M. 2004, *Measurement of Inhomogeneous Deformation Behavior Arising in SMA*. J. Soc. Mat. Sci., Japan, 53, 9, 999–1005.

Brinson L.C., Schmidt I., Lammering R. 2004, *Stress-indeced transformation behavior of a polycrystalline NiTi shape memory alloy: micro and macromechanical investigation via in situ optical microscopy*. J. Mech. Phys. Solids, 52, pp. 1549–1571.

Daly S., Ravichandran G., Bhattacharya K. 2007, *Stress-induced martensitic phase transformation in thin sheets of Nitinol*. California Institute of Technology, Acta Materialia, 55, pp. 3593–3600.

Favier D., Louche H., Schlosser P., Orgeas L., Vacher P., Debove L. 2007, *Homogeneous and heterogeneous deformation mechanisms in austenitic polycrystalline Ti-50.8 at.%Ni thin tube under tension. Investigation via temperature and strain fields measurements*. Acta Materialia, 55, pp. 5310–5322.

Pieczyska E.A., Tobushi Hisaaki, Nowacki W.K., Gadaj S.P., Sakuragi Toshimi 2007, *Subloop Deformation Behavior of TiNi Shape Memory Alloy Subjected to Stress-Controlled Loadings*, Materials Transactions. vol. 48, No 10, pp. 2679–2686.

Pieczyska E. 2010, *Activity of Stress-Induced Martensite Transformation in Shape Memory Alloy Studied by Infrared Technique*, Journal of Modern Optics. vol. 57, no. 18, pp. 1700–1707.

He Y.J., Sun Q.P. 2010, *Rate-dependent domain spacing in a stretched NiTi strip*. Int. J. Solids Struct., 47, pp. 2775–2783.